Roller embossing process for the replication of shark-skin-inspired micro-riblets

Chunfang Guo, Qianqian Tian, Hairui Wang, Jianxing Sun, Liqun Du, Minjie Wang, Danyang Zhao ✉

Key Laboratory for Precision & Non-traditional Machining Technology of Ministry of Education, Dalian University of Technology, Dalian 116024, People's Republic of China
✉ *E-mail: zhaody@dlut.edu.cn*

Published in Micro & Nano Letters; Received on 22nd November 2016; Revised on 9th February 2017; Accepted on 28th February 2017

The riblet structures of shark skin have a significant biological function for drag reduction, which has been verified. However, it is difficult to fabricate large-scale bionic shark skin surface with high precision and low cost. The real shark skin micro-riblets were first measured and approximately simplified to obtain shark-skin-inspired micro-riblets. Numerical simulations were performed to explore the drag-reduction effect of the micro-riblets surface. According to the simplified micro-riblets, a nickel mould with negative micro-structures was manufactured by Ultra-Violet Lithographie, Galvanoformung and Abformung technique. Roller embossing process was adopted to replicate shark-skin-inspired micro-riblets, capable of transferring the micro-riblets to polyvinyl chloride (PVC) and polyethylene terephthalate (PET) films. After embossing experiments, the effect of process parameters on roller embossing qualities including mould temperature, rolling pressure and rolling speed, evaluated by the depths of riblets embossed on the polymer films, were investigated. The results showed that the roller embossing process is a feasible and effective method to continuously replicate shark-skin-inspired micro-riblets on polymer substrates. Moreover, the optimal process parameters were determined, including mould temperatures of 70°C (for PVC) and 60°C (for PET), compression ratios of 1.22 (for PVC) and 1.53 (for PET) and rolling speed of 1 r/min.

1. Introduction: With the spread of world energy crisis, the drag-reduction technology of ships and aircrafts plays an increasingly significant role as an effective approach to saving energy. Nature is full of examples of structures, materials and surfaces whose traits can be exploited for engineering applications. For instance, the skin of fast-swimming sharks protects against biofouling and reduces the drag experienced by sharks as they swim in water. The tiny scales covering the skin of fast-swimming sharks, known as dermal denticles, are shaped like small riblets and aligned in the direction of fluid flow [1]. Researchers have already made some achievements in the drag-reduction mechanisms of shark skin surface through experimental and numerical studies [2, 3]. Shark-skin-inspired riblets have been verified to provide drag-reduction effect up to 10% [4]. For better similarity with real shark skin and easy fabrication, researchers usually optimise the structures of shark-skin-inspired riblets [5, 6]. The relationship between the drag-reduction mechanisms and the geometry of riblets has been investigated. The optimisation of shark skin-inspired riblets has also been studied experimentally to reduce drag in closed channel flow [7, 8]. With water and air, riblets show an improved pressure drop reduction in turbulent versus laminar flow, presumably due to the lifting and pinning of vortices. According to the special structures, the hydrophobic property of shark-skin-inspired micro-riblets has been studied and a new hydrophobic model was proposed [9].

Researchers have also studied the replication approaches of shark skin surface. For its complex structures, the real shark skin is usually replicated on polymer substrates by moulding techniques, such as micro-embossing process [10] and vacuum casting method [11]. Recently, three-dimensional printing technique has also been used to carry out the design, fabrication and hydrodynamic testing of a synthetic and flexible shark skin membrane [12]. Microfabrication techniques are commonly used to fabricate micro-structures on metal substrates, including micro-cutting, micro-un-traditional machining and Lithographie, Galvanoformung and Abformung-based methods [13, 14]. To broaden the application range, the continuous replication of shark-skin-inspired micro-riblets in large scale is still required, especially on polymer films. An efficient replication method of micro-structures on polymer substrates has been developed by researchers, known as roller embossing process [15, 16]. The continuous roll-to-roll embossing technique can provide a solution for high-speed large-area micro-scale patterning with greatly improved throughput [17, 18].

In this Letter, the real shark skin micro-structures were first measured and approximately simplified. Numerical simulations were performed to verify the drag-reduction effect of the micro-riblets surface in turbulent flow. According to the simplified micro-riblets, a nickel mould with negative micro-structures was manufactured by Ultra-Violet Lithographie, Galvanoformung and Abformung technique. Roller embossing process was adopted to continuously replicate shark-skin-inspired micro-riblets on polymer films, and embossing experiments were conducted under different process conditions. After experiments, the depths of embossed micro-riblets were measured to investigate the effect of process parameters, including mould temperature, rolling pressure and rolling speed, on roller embossing qualities.

2. Structure simplification: Shark skin is composed of many small scales arranged in an interlocking array. The morphology of shark skin surface taken by scanning electron microscope is shown in Fig. 1*a*. The cross-section profile of the scale measured by CLI 2000 mechanical stylus surface profiler is presented in Fig. 1*b*, indicating that the shark skin scale has longitudinal ribs of different length and height.

To approximate the real shark skin scale riblets, the scale was simplified as rhombus shape and the cross-section profile of shark skin micro-riblets was represented by trapezoid structures with the same height. The shark-skin-inspired micro-riblets are illustrated in Fig. 1*c*. As shown in Fig. 1*d*, the cross-section profile of shark-skin-inspired micro-riblets mainly contains the following dimensions: riblet space f, riblet depth h, riblet width w and riblet slope θ. In this Letter, the simplified dimensions are determined as follows: riblet space f of 100 μm and riblet depth h of 50 μm. Confined by other dimensions, riblet width w was determined as 50 μm from the view of symmetry. Affected by specific processing method, riblet slope θ was determined as 0° considering the following mould manufacture technique.

Numerical simulations were performed to explore the drag-reduction effect of the simplified shark skin in turbulent flow. Computational models of lower shark skin surface and

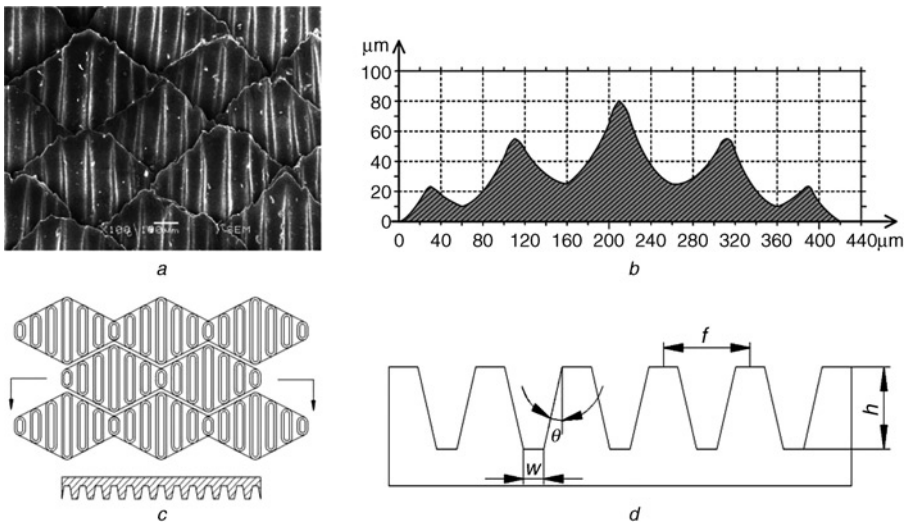

Fig. 1 *Structure simplification of shark skin surface*
a Scanning microscopy image of shark skin surface
b Cross-section profile of shark skin scale
c Shark-skin-inspired micro-riblets
d Cross-section profile of shark-skin-inspired micro-riblets

shark-skin-inspired micro-riblets surface were built, respectively, and each of them was compared with upper smooth surface, shown in Figs. 2*a* and *c*. The models were meshed with refined grids near the upper smooth wall and lower non-smooth wall. In addition, the boundary conditions were treated as follows: (i) the flow inlet and outlet of the computational flow field were set as in a periodical boundary condition; (ii) the side boundary of the computational flow field was set as in a symmetry condition; (iii) the upper smooth wall and lower non-smooth wall were set as in no-slip boundary condition. Considering the fast-swimming velocity of shark in water is about 16 m/s, the fluid velocity in the simulation was set from 10 to 20 m/s, with an interval of 2 m/s.

After calculation, the integral of shear stress on the shark skin surface, micro-riblets surface and their corresponding smooth surfaces were exported. The shear stress distributions are shown in Figs. 2*b* and *d*. The results showed that the integral of shear stresses on these two surfaces are much less than their corresponding smooth surfaces. The drag-reduction rate can be defined as $r = ((t_s - t)/t_s) \times 100\%$, where t_s is the shear stress on smooth surface, and t is the shear stress on the shark skin surface or micro-riblets surface [5]. The relationship between drag-reduction rate and fluid velocity of these two surfaces are shown in Fig. 3. The shark-skin-inspired micro-riblets surface is verified to have significant drag-reduction effect, indicating the reasonable simplification for large-scale replication of shark skin surface.

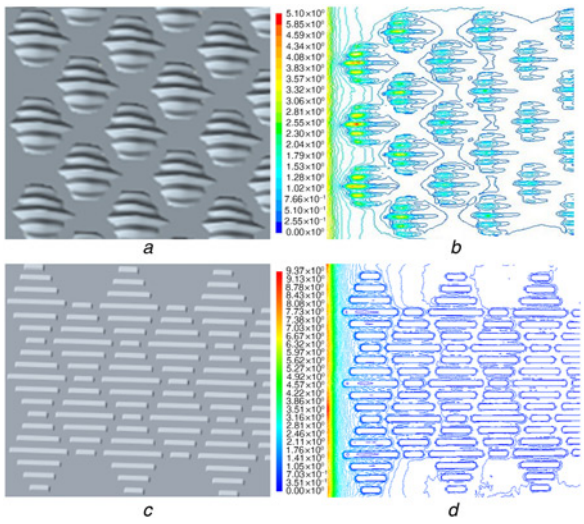

Fig. 2 *Computational models and shear stress distributions*
a, *b* Shark skin surface
c, *d* Micro-riblets surface

3. Manufacturing of roller embossing mould: To replicate large-scale shark-skin-inspired micro-riblets by roller embossing process, a metal mould with negative micro-structures was needed. In micro-fabrication field, UV-LIGA technique is widely used to produce micro-structures on metal substrates, with the advantages of high precision and broad material range. Thus, UV-LIGA technique was adopted to fabricate a nickel mould for roller embossing process. According to the dimensions of simplified micro-riblets, the corresponding dimensions of the mould were determined. The channel space, channel width and channel depth of the mould micro-structures were designed to be 100, 50 and 50 μm, respectively. As mentioned in above paragraphs, restricted by the mould manufacture method, the channel slope was selected to be 0°. Based on the dimensions of the mould to be produced, a mask was first fabricated. During the pretreatment, Ni201 with thickness of 0.5 mm was chosen as the

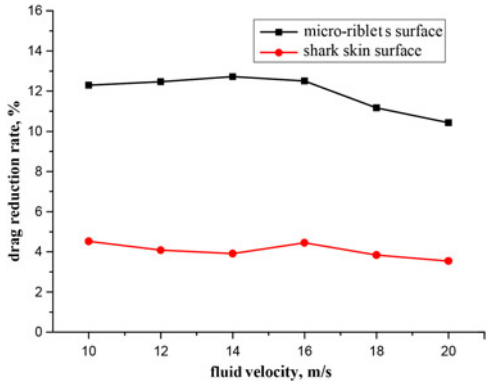

Fig. 3 *Relationship between drag-reduction rate and fluid velocity*

doi: 10.1049/mnl.2016.0759

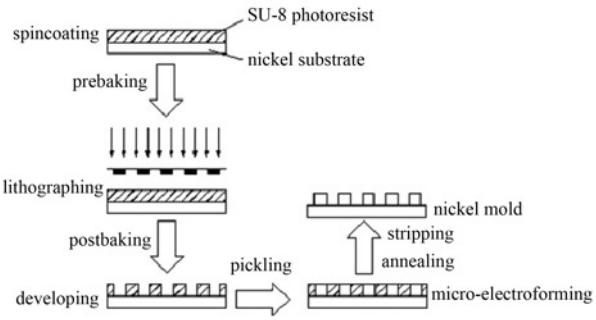

Fig. 4 *UV-LIGA process procedures*

nickel substrate, and bonded with a nickel plate of 3.0 mm to avoid the deformation of the thin substrate. The nickel substrate was also polished to remove surface rust and oxide layer. The UV-LIGA procedures are schematically shown in Fig. 4, which mainly contain pretreating, spincoating, prebaking, lithographing, postbaking, developing, pickling, micro-electroforming, annealing and stripping. After being separated with the nickel plate and washed by acetone solution, the nickel mould with negative micro-structures was fabricated. Shown in Fig. 5, the nickel mould fabricated by UV-LIGA method appears to be complete in structure and clear in profile without cracks or viscose, exhibiting certain independence and regularity.

4. Roller embossing experiments

4.1. Materials and equipment: Polyvinyl chloride (PVC) and polyethylene terephthalate (PET) films were used to perform the roller embossing experiments. Properties of the polymer films are illustrated in Table 1. The experimental equipment was XW-305C double-roller embossing machine, and the mirror diameter of each roller was 120 mm.

4.2. Experimental process

(i) The smooth surface of the nickel mould was burnished by sand paper, coated by a thin layer of glue, and then attached to the roller surface. The roller embossing process is schematically shown in Fig. 6.

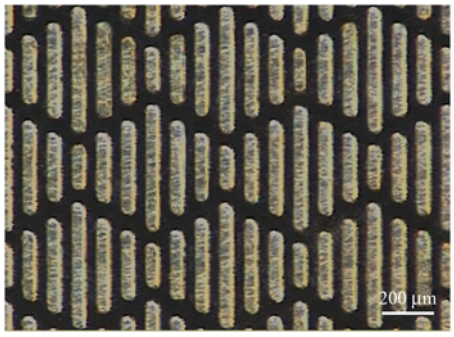

Fig. 5 *Image of the nickel mould*

Table 1 Properties of the PVC and PET films

Properties	PVC	PET
thickness, mm	0.20	0.14
glass transition temperature T_g, °C	80	70
melting temperature T_m, °C	170–180	250–265
shrink rate, %	0.6–1.5	1.2–2.0

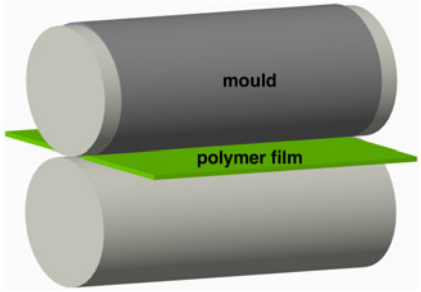

Fig. 6 *Schematic diagram of the roller embossing process*

(ii) The 0.20 mm thick PVC films and 0.14 mm thick PET films were clipped to suit the nickel mould, cleaned to remove surface stains, then wiped and dried in the air.

(iii) Considering T_g of PVC and PET are about 80 and 70°C, respectively. The temperatures of the pressure roller contacting with the films were set as 80°C (for PVC) and 70°C (for PET). The temperature of the embossing roller with nickel mould was set in the range of room temperature to 90°C. Besides, the two rollers were set at the same rotate speed from 1.0 to 3.5 r/min.

(iv) The thickness of the nickel mould and glue layer was measured to be 0.37 ± 0.04 and 0.10 ± 0.02 mm by vernier caliper, respectively. Therefore, the total mould–glue–film thicknesses comprising the nickel mould, glue layer and the polymer films were about 0.67 mm (for PVC) and 0.61 mm (for PET). During the experimental process, the pressure between the rollers was indirectly adjusted by changing the roller space and measured using a dimensionless compression ratio, defined as the ratio between the total mould–glue–film thickness and the roller space.

(v) Single variable method was used to perform the experiments. The average depth of riblets on the films embossed at varying mould temperature was measured while the compression ratio and rolling speed were certain to determine the optimal mould temperature. Similarly, the optimal compression ratio and rolling speed were determined.

The values of mould temperature, roller space, compression ratio and rolling speed used in roller embossing experiments are illustrated in Table 2.

5. Results and discussion: The polymer films embossed under mould temperatures of 70°C (for PVC) and 60°C (for PET), compression ratios of 1.22 (for PVC) and 1.53 (for PET) and rolling speed of 1.0 r/min are shown in Fig. 7. Seen from Figs. 7*a* and *c*, the nickel mould can replicate shark-skin-inspired micro-riblets on polymer films neatly. However, the embossed micro-riblets are not completely consistent with the original

Table 2 Values of process parameters used in roller embossing experiments

Process parameters	PVC	PET
mould temperature, °C	30, 40, 50, 60, 70, 80, 90	30, 40, 50, 60, 70, 80, 90
roller space, mm	0.65, 0.62, 0.60, 0.57, 0.55, 0.50	0.51, 0.48, 0.45, 0.42, 0.40, 0.38
compression ratio	1.03, 1.08, 1.12, 1.18, 1.22, 1.34	1.20, 1.27, 1.36, 1.45, 1.53, 1.61
rolling speed, r/min	1.0, 1.5, 2.0, 2.5, 3.0, 3.5	1.0, 1.5, 2.0, 2.5, 3.0, 3.5

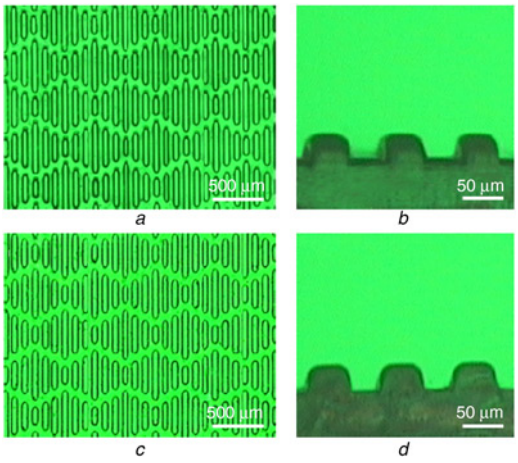

Fig. 7 *Polymer films with shark-skin-inspired micro-riblets*
a PVC film
b Cross-section shape of PVC film
c PET film
d Cross-section shape of PET film

micro-structures on the nickel mould. Shown in Figs. 7*b* and *d*, the average depths of riblets on PVC and PET films are 43.8 and 37.5 μm respectively, indicating that the depths of embossed micro-riblets are smaller than the depth of mould structures, and PVC is much preferable than PET. During the roller embossing process, viscoelastic polymer is extruded into the recessed portion of the nickel mould, then move upward along the sidewall of the recessed portion. If the embossing time is adequate, the polymer will be extruded continuously, and then the polymer inside the cavity will rise under the high pressure. However, the rolling speed during the embossing experiments could not be excessive low, and the polymer films get separated with the mould before the filling process is accomplished. Elastic recovery of the polymer takes place after mould–polymer separation, which results in the width and slope deformation of polymer structures.

The filling of polymer in mould cavity during embossing can be approximately described as one-dimensional flow between two infinitely long plates. The simplified filling model is schematically shown in Fig. 8, where W is the width of mould cavity and H is the depth of the mould cavity. Since the polymer mass is small, the effect of gravity can be ignored. Assuming the polymer flow is viscous, the flow equation of polymer in Z direction can be described by the Navier–Stokes equation

$$\frac{\partial P}{\partial z} = \eta \frac{\partial^2 v_z}{\partial x^2}. \tag{1}$$

where $\partial P/\partial z$ is the pressure gradient in Z direction; ∂z is the flow velocity of polymer in Z direction; η is the viscosity of polymer. Assuming the boundary condition of no-slip wall, (2) can be derived from integrating (1)

$$v_z = \frac{\partial P}{\partial z}\frac{1}{2\eta}\left(x^2 - \frac{W^2}{4}\right). \tag{2}$$

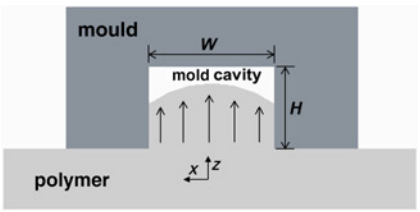

Fig. 8 *Filling model of polymer in mould cavity*

According to Hertz contact theory, the contact cycle t_c between a specific micro-structure on the mould and the polymer film during the roller embossing process can be written as: $t_c = a/v$, where a is the contact length and v is the linear velocity of polymer film. Then the average velocity of the polymer front in a contact cycle can be calculated as

$$\bar{v}_z = \frac{1}{t_c}\frac{1}{W}\int_0^{t_c}\int_{-(W/2)}^{W/2} v_z \,\mathrm{d}x\,\mathrm{d}t = \frac{\bar{P}}{\Delta H}\frac{W^2}{12\eta}. \tag{3}$$

where ΔH is the filling height of the polymer, $\bar{P}$ is the average pressure in the contacting region of the mould and the polymer in a contact cycle. Therefore, the filling height of the polymer ΔH in a contact cycle can be expressed as

$$\Delta H = \bar{v}_z t_c = \frac{\bar{P}}{\Delta H}\frac{W^2}{12\eta}\frac{a}{v}. \tag{4}$$

Finally, the filling height of the polymer in the mould cavity ΔH can be calculated by

$$\Delta H = W\left(\frac{\bar{P}a}{12\eta v}\right)^{1/2}. \tag{5}$$

5.1. Effect of mould temperature: To study the effect of mould temperature on roller embossing quality, the roller spaces were set as 0.55 mm (for PVC) and 0.40 mm (for PET) and the corresponding compression ratios were 1.22 and 1.53, respectively. The rolling speed was set as 1.0 r/min and the mould temperature was adjusted from 30 to 90°C with the interval of 10°C. The average depth of riblets on the PVC and PET films embossed at varying mould temperatures is shown in Fig. 9*a*. Since the polymer in mould cavity cools rapidly and the drag of polymer flow front increases under lower mould temperature, it is difficult for polymer to fill mould cavity. With mould temperatures increasing to 70°C (for PVC) and 60°C (for PET), the temperature difference and heat exchange between the mould and the films decrease, thus the polymer maintains good liquidity to accomplish preferable filling. As can be explained by (5), the higher mould temperature maintains the lower viscosity of polymer η, leading to higher filling height ΔH. However, when the mould temperature reaches T_g or above, the depth of micro-riblets is smaller than that embossed at mould temperature slightly below T_g. This is mainly because high mould temperature leads to obvious polymer deformation recovery after the separation of mould and polymer without adequate cooling. Therefore, roller embossing process should be accomplished under mould temperature about 10°C below T_g of the polymer.

5.2. Effect of rolling pressure: To study the effect of rolling pressure on roller embossing quality, the mould temperatures were set as 70°C (for PVC) and 60°C (for PET), the rolling speed was set as 1.0 r/min, and the compression ratios were adjusted by regulating the roller space. The average depth of riblets on the PVC and PET films embossed under varying rolling pressures is shown in Fig. 9*b*. A dimensionless compression ratio is used to measure the rolling pressure. The compression ratio and the rolling pressure between the mould and film increase when the roller space decreases. As Fig. 9 shows, the depth of the micro-riblets on polymer films increases with the increase of rolling pressure. Seen from (3) and (5), the higher average pressure $\bar{P}$ increases the filling velocity of polymer in mould cavity during the contact cycle, thus leading to higher filling height ΔH. However, the compression ratio should not be higher than 1.61, in order to protect the mould and polymer films.

doi: 10.1049/mnl.2016.0759

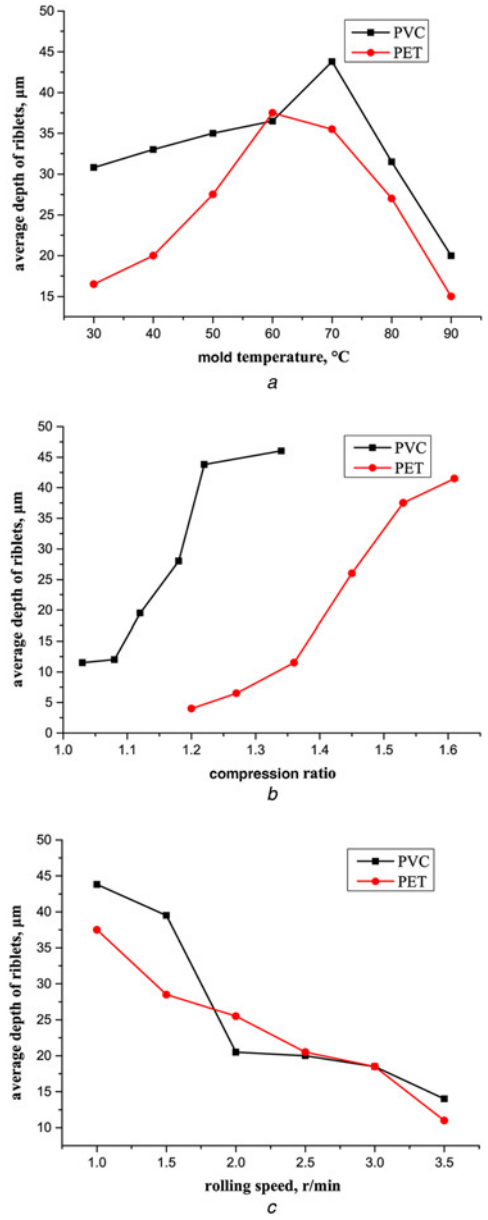

Fig. 9 *Average depth of riblets on the PVC and PET films embossed at varying mould temperatures, compression ratio and rolling speed*
a Curves between average depth of riblets and mould temperature
b Curves between average depth of riblets and compression ratio
c Curves between average depth of riblets and rolling speed

5.3. Effect of rolling speed: To study the effect of rolling speed on roller embossing quality, the mould temperatures were set as 70°C (for PVC) and 60°C (for PET), the roller spaces were set as 0.55 mm (for PVC) and 0.40 mm (for PET) with corresponding compression ratios of 1.22 and 1.53, respectively, and the rolling speeds were adjusted from 1.0 to 3.5 r/min with the interval of 0.5 r/min. The average depth of riblets on the PVC and PET films embossed at varying rolling speeds is illustrated in Fig. 9*c*. The depth of the micro-riblets on polymer films decreases with the increase of rolling speed. This is mainly because the contact cycle between the mould and polymer film gets shorter when the rolling speed increases. Then, the polymer has less time to fill the mould cavity, so the filling is inadequate. As (5) indicates, the lower rolling speed v leads to higher filing height ΔH. Nevertheless, the rolling speed should not be lower than 1 r/min, to ensure the embossing efficiency and avoid the stuck of embossing rollers.

6. Conclusions: In this Letter, the real shark skin micro-riblets were measured and approximately simplified to realise large-scale replication. Numerical simulations were performed to verify the drag-reduction effect of the shark-skin-inspired micro-riblets. According to the simplified micro-riblets, UV-LIGA technique was adopted to fabricate a nickel mould with negative micro-structures. The mould appeared to be complete in structure and clear in profile without cracks or viscose and satisfied the experimental requirements, verifying the feasibility of UV-LIGA technique to fabricate roller embossing mould.

The roller embossing process could continuously replicate shark-skin-inspired micro-riblets on polymer films, and PVC is much preferable than PET. Though, the embossed micro-riblets were not completely consistent with the mould micro-structures. The increase of mould temperature can improve the polymer liquidity and facilitate the filling of polymer into mould cavity. However, high mould temperature also leads to apparent polymer deformation recovery after the separation of mould and polymer without adequate cooling, since embossing and demoulding occur at the same temperature during the roller embossing process. The increase of rolling pressure can increase the filling velocity of polymer in mould cavity during the contact cycle, leading to higher filling height. The contact cycle between the mould and polymer increases with the decreasing rolling speed. Thus, the polymer has more time to fill the mould cavity at lower rolling speed, and the filling is more adequate. In this Letter, the roller embossing process is preferable to be accomplished at mould temperatures of 70°C (for PVC) and 60°C (for PET), compression ratios of 1.22 (for PVC) and 1.53 (for PET), and rolling speed of 1 r/min.

7. Acknowledgment: This work was supported by the National Natural Science Foundation of China under the grant no. 51275071.

8 References

[1] Ball P.: 'Engineering shark skin and other solutions', *Nature*, 1999, **400**, pp. 507–509
[2] Lee S.J., Lee S.H.: 'Flow field analysis of a turbulent boundary layer over a riblet surface', *Exp. Fluids*, 2001, **30**, (2), pp. 153–166
[3] Zhang D.Y., Luo Y.H., Li X., *ET AL.*: 'Numerical simulation and experimental study of drag-reducing surface of a real shark skin', *J. Hydrodyn.*, 2011, **23**, (2), pp. 204–211
[4] Bechert D.W., Bruse M., Hage W.: 'Experiments with three-dimensional riblets as an idealized model of shark skin', *Exp. Fluids*, 2000, **28**, (5), pp. 403–412
[5] Dean B., Bhushan B.: 'Shark-skin surfaces for fluid-drag reduction in turbulent flow: a review', *Philos. Trans. R. Soc. A*, 2010, **368**, (1929), pp. 4775–4806
[6] Bixler G.D., Bhushan B.: 'Fluid drag reduction with shark-skin riblet inspired microstructured surfaces', *Adv. Funct. Mater.*, 2013, **23**, (36), pp. 4507–4528
[7] Bixler G.D., Bhushan B.: 'Bioinspired rice leaf and butterfly wing surface structures combining shark skin and lotus effects', *Soft Mat.*, 2012, **8**, (44), pp. 11271–11284
[8] Bixler G.D., Bhushan B.: 'Shark skin inspired low-drag microstructured surfaces in closed channel flow', *J. Colloid Interface Sci.*, 2013, **393**, pp. 384–396
[9] Zhao D.Y., Tian Q.Q., Wang M.J., *ET AL.*: 'Study on the hydrophobic property of shark-skin-inspired micro-riblets', *J. Bionic Eng.*, 2014, **11**, (2), pp. 296–302
[10] Han X., Zhang D.Y., Li X., *ET AL.*: 'Bio-replicated forming of the biomimetic drag-reducing surfaces in large area based on shark skin', *Chin. Sci. Bull.*, 2008, **53**, (10), pp. 1587–1592
[11] Zhao D.Y., Huang Z.P., Wang M.J., *ET AL.*: 'Vacuum casting replication of micro-riblets on shark skin for drag-reducing applications', *J. Mater. Process. Technol.*, 2012, **212**, (1), pp. 198–202
[12] Wen L., Weaver J.C.: 'Biomimetic shark skin: design, fabrication and hydrodynamic function', *J. Exp. Biol.*, 2014, **217**, (10), pp. 1656–1666
[13] Heckele M., Schomburg W.K.: 'Review on micro molding of thermoplastic polymers', *J. Micromech. Microeng.*, 2003, **14**, (3), pp. R1
[14] Peng L.F., Deng Y.J., Yi P.Y., *ET AL.*: 'Micro hot embossing of thermoplastic polymers: a review', *J. Micromech. Microeng.*, 2013, **24**, (1), p. 013001

[15] Yeo L.P., Ng S.H., Wang Z., *ET AL.*: 'Micro-fabrication of polymeric devices using hot roller embossing', *Microelectron. Eng.*, 2009, **86**, (4), pp. 933–936
[16] Ng S.H., Wang Z.F.: 'Hot roller embossing for microfluidics: process and challenges', *Microsyst. Technol.*, 2009, **15**, (8), pp. 1149–1156
[17] Ahn S.H., Guo L.J.: 'Large-area roll-to-roll and roll-to-plate nanoimprint lithography: a step toward high-throughput application of continuous nanoimprinting', *ACS Nano*, 2009, **3**, (8), pp. 2304–2310
[18] Tsao C.W., Chen T.Y., Woon W.Y., *ET AL.*: 'Rapid polymer microchannel fabrication by hot roller embossing process', *Microsyst. Technol.*, 2012, **18**, (6), pp. 713–722

doi: 10.1049/mnl.2016.0759